Int. J. Heat Mass Transfer. Vol. 15, pp. 1537–1552. Pergamon Press 1972. Printed in Great Britain

THE ENHANCEMENT OF HEAT TRANSFER BY WAVES IN STRATIFIED GAS–LIQUID FLOW

DAVID P. FRISK and E. JAMES DAVIS

Chemical Engineering Department, Clarkson College of Technology, Potsdam, New York, U.S.A.

(*Received* 22 *July* 1971 *and in revised form* 12 *November* 1971)

Abstract—An experimental investigation of heat transfer from a flat plate to horizontal cocurrent air–water flow has been carried out to assess the effects of the different flow regimes on the effectiveness of the heat transfer. The results for smooth liquid film flow and two-dimensional wavy flow of the liquid phase are shown to agree with the theoretical analysis of heat transfer to smooth films. Three-dimensional waves and roll waves are shown to increase the Nusselt number (compared with smooth films) by more than 100 per cent. By using a surface-active agent to stabilize the flow direct comparison between wavy flow heat transfer and smooth flow heat transfer is obtained. At sufficiently low gas phase Reynolds numbers and at sufficiently high wall heat fluxes Rayleigh-like instability due to buoyant forces is shown to occur.

NOMENCLATURE

Roman letters

A_n, eigenconstants in equation (6);

B, Gr/Re_{L_i} ratio of the Grashoff and Reynolds numbers;

g, gravitational acceleration constant [cm/s^2];

Gr, $\delta^3\rho_L^2 g\beta(T_w - T_b)/\mu_L^2$, Grashoff number [dimensionless];

$\bar{h}$, average heat transfer coefficient [J/m^{2}s°K];

$J_{\frac{1}{3}}(z)$, $J_{-\frac{1}{3}}(z)$, Bessel functions;

k, thermal conductivity [J/ms°K];

K_1, K_2, integration constants;

Nu, $q_w\delta/k(T_w - T_b)$, Nusselt number [dimensionless];

Pe, $\delta U_i/\alpha$, Péclét number [dimensionless];

Po, $-\psi\delta^2/2\mu U_i$, Poiseuille number [dimensionless];

Q, volumetric flow rate [cm^3/s];

Re_G, Q_G/Wv_G, Reynolds number [dimensionless];

Re_L, Q_L/Wv_L, liquid phase Reynolds number [dimensionless];

Re_{L_i}, $\delta U_i/v_L$, liquid phase Reynolds number [dimensionless];

T, temperature [°K];

T_b, mixed mean liquid film temperature [°K];

T_0, inlet temperature [°K];

T_w, wall temperature [°K];

u, velocity [cm/s];

u_i, velocity for pure Poiseuille film flow [cm/s];

U_i, velocity for pure Couette flow [cm/s];

W, tunnel width [cm];

x, axial coordinate;

y, transverse coordinate.

Greek letters

α, thermal diffusivity [cm^2/s];

β, coefficient of thermal expansion [°K^{-1}];

δ, liquid film thickness [cm];

ζ, dimensionless transverse coordinate;

θ, $(T - T_0)/(q_w\delta/k)$, dimensionless temperature;

θ_∞, asymptotic dimensionless temperature distribution;

λ_n, eigenvalues;

μ, viscosity [g/cms];

ν, kinematic viscosity [cm^2/s];

ξ, dimensionless axial coordinate;

ρ, density [g/cm^3];
σ, surface tension [dynes/cm];
τ_i, interfacial shear stress [dyne/cm^2];
ψ, pressure gradient [dyne/cm^3];
Ψ_n, eigenfunction.

Subscripts

G, refers to the gas phase;
i, refers to the gas–liquid interface;
L, refers to the liquid phase;
0, refers to the inlet;
w, refers to the wall.

INTRODUCTION

WHEN a gas and a liquid flow concurrently in a channel or conduit the fluid mechanics is complicated by the variety of flow patterns that can occur. The flow patterns depend not only on the Reynolds numbers of the two phases but also on the interfacial tension and other parameters that are not usually significant for single phase flow. Since the flow field greatly affects heat and mass transfer rates it is to be expected that heat and/or mass transfer to two-phase flows depend upon the flow regimes encountered.

Horizontal flow of gas–liquid mixtures in a duct of large aspect ratio (width to height) has been widely studied to elucidate some of the characteristics of two-phase flow. Hanratty and Engen [1] identified the flow regimes that are observed for a fixed liquid flow rate as the gas flow rate is increased. They are: (1) smooth interface, (2) two-dimensional waves, (3) three-dimensional waves, (4) roll waves and (5) atomization, i.e. dispersion in the gas phase of liquid droplets torn from the film. Ellis and Gay [2], van Rossum [3], Smith and Tait [4] and Davis [5] also observed and studied these wave regimes.

Although the interfacial structures reported by the above investigators are reproducible and well defined the addition of even trace amounts of surface-active agents substantially changes the interfacial profiles and the transitions from one regime to another. Hanratty and Hershman [6] reported the effects of a surfactant, sodium lauryl sulfate, on the transition to two- and three-dimensional waves for air–water flow. They found that even the roll wave transition is shifted to higher gas phase Reynolds numbers when the liquid film is contaminated. Davis and Cooper [7] used a soluble surfactant to stabilize the liquid film in their study of heat transfer to horizontal air–water flow with a smooth interface, and Craik [8] and Smith and Craik [9] theoretically and experimentally examined the stability of a liquid film containing a soluble surfactant when an air stream flows over the film. The latter investigators found that at large liquid Reynolds numbers the stability is enhanced due to increased viscous dissipation in the viscous layer just within the liquid surface, and at small liquid Reynolds numbers surface elasticity may be destabilizing. Recently Narasimhan and Davis [10, 11] studied the effects of surfactants on the interfacial structure in horizontal air–water flow, finding that the two- and three-dimensional wave regimes are frequently replaced by a flow regime involving wave patches on an otherwise smooth film. The wave patch regime occurs over a fairly wide range of gas and liquid flow rates.

It is the purpose of the present paper to report the results of heat transfer measurements associated with the various flow regimes discussed above. Although Davis and Cooper provided some data on heat transfer to horizontal wavy film flow, their results were largely confined to smooth film flow. The present work extends and amplifies the study of Davis and Cooper.

RELATED MASS AND HEAT TRANSFER STUDIES

Since the 1954 study of Emmert and Pigford [12] on the absorption of gases by both rippling and smooth falling liquid films there has been considerable interest shown in mass transfer to liquid film flow [13–36]. But most of these studies are concerned with the enhancement of mass transfer at the gas–liquid or liquid–liquid [26] interface due to ripples or standing waves

[20, 27]. It is generally agreed that interfacial mass transfer is greatly enhanced by wave motion.

Mass transfer at the solid–liquid boundary is another matter. Using an inclined plate, part of which was benzoic acid, Kramers and Kreyger [16] studied mass transfer at the wall for short surfaces. Their results are consistent with laminar boundary layer theory, indicating that the wave motion did not penetrate to the wall. Stirba and Hurt [15] used a longer soluble surface in a similar study of vertically falling films. The increased mass transfer rates (compared with smooth films) were considered to be due to wave induced turbulence in the film. Iribarne *et al.* [24] and Wragg *et al.* [34] used electrochemical techniques to study mass transfer at a wall with film flow. They found their results to be in agreement with the Leveque solution for laminar flow, which suggests that for short sections the wave motion has no effect on the flow field at the wall. Oliver and Atherinos [35] drew the same conclusions from their study of mass transfer from an inclined soluble wall to a liquid film. The latter researchers made dye tracer studies which showed that the surface ripples had no effect on the flow of liquid adjacent to the solid surface.

Relatively little work on heat transfer specifically to wavy film flow has been carried out. Bays and McAdams [37], Williams *et al.* [38] and Chand and Rosson [39] studied heat transfer to wavy vertical film flow, reporting that ripples enhance heat transfer from the wall by only 20–30 per cent. Fedotkin and Firisyuk [40] reported enhancements of 20–130 per cent in their study using an inclined heated plate, but they provided no information about the wave characteristics. Inducing surface waves by means of an electric field Choi [4] found that the vertical condensation heat transfer coefficient was increased by as much as 100 per cent over smooth film values. Davis and Cooper [7] also measured substantial enhancement of heat transfer by wave motion in horizontal two-phase flow.

In a theoretical analysis of heat transfer between a solid wall and a wave O'Brien [42] used a Gerstner wave model of the flow field to predict, at most, a 100 per cent increase in heat transfer compared with smooth films.

ANALYSIS

The temperature field in a smooth horizontal liquid film flowing under the influence of a pressure gradient and the shear of a concurrently flowing gas phase is described by the convective diffusion equation

$$u\frac{\partial T}{\partial x} = \alpha\left(\frac{\partial^2 T}{\partial y^2} + \frac{\partial^2 T}{\partial x^2}\right). \tag{1}$$

The coordinates and a schematic diagram of the system are shown in Fig. 1. The velocity distribution in the liquid film is a function of the pressure gradient ψ in the conduit as well as the interfacial shear τ_i exerted by the turbulent gas phase on the liquid, i.e.

$$u = \frac{\psi}{2\mu}(y^2 - 2\delta y) + \frac{\tau_i y}{\mu} \tag{2}$$

where δ is the liquid film thickness.

If U_i is the interfacial velocity for pure Couette flow ($\psi = 0$) of the liquid film and u_i is the interfacial velocity for pure Poiseuille flow ($\tau_i = 0$) then the velocity distribution may be written

$$\frac{u}{U_i} = \frac{u_i}{U_i}\left(2\frac{y}{\delta} - \frac{y^2}{\delta^2}\right) + \frac{y}{\delta}. \tag{3}$$

If the pressure gradient is sufficiently small compared with the interfacial shear, i.e. if $u_i/U_i \ll 1$, Equation (3) reduces to a linear velocity profile. This is generally the case for the experiments discussed below. The parameter u_i/U_i can be recognized as the Poiseuille number, $Po \equiv -\psi\delta^2/2\mu U_i$.

Introducing dimensionless variables

$$\zeta = \frac{y}{\delta},\ \xi = \frac{x}{\delta Pe} \text{ and } \theta = \frac{(T - T_0)}{(q_w\delta/k)}$$

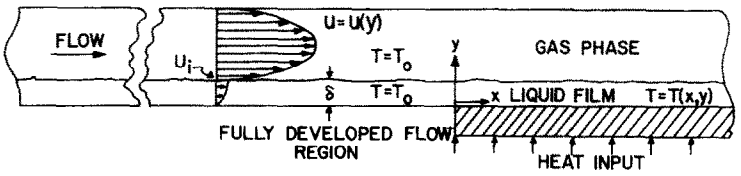

FIG. 1. The system and coordinates under consideration.

where $Pe \equiv \delta U_i/\alpha$, and incorporating equation (3) in equation (1) we obtain

$$[Po(2\zeta - \zeta^2) + \zeta]\frac{\partial\theta}{\partial\xi} = \frac{\partial^2\theta}{\partial\zeta^2} + \frac{1}{Pe^2}\frac{\partial^2\theta}{\partial\xi^2}. \quad (4)$$

The dimensionless temperature is normalized by the factor $q_w\delta/k$ because the experiments were made at constant wall heat flux q_w.

The solution of equation (4) has been discussed in considerable detail by Davis [43] elsewhere. For $Pe > 100$ the axial conduction term can be neglected, and when $Po \ll 1$ also, equation (4) reduces to

$$\zeta\frac{\partial\theta}{\partial\xi} = \frac{\partial^2\theta}{\partial\zeta^2}, \quad (5)$$

which was discussed by Davis and Cooper. They presented the solution of equation (5) for several sets of boundary conditions at the wall and at the interface.

The solution of equation (5) is

$$\theta = \theta_\infty + \sum_{n=1}^{\infty} A_n\Psi_n(\zeta)\exp(-\lambda_n^2\xi) \quad (6)$$

where θ_∞ is the asymptotic temperature distribution, and the eigenfunctions are given by

$$\Psi_n(\zeta) = K_1\lambda_n^{\frac{1}{3}}\sqrt{\zeta}J_{\frac{1}{3}}(\tfrac{2}{3}\lambda_n\zeta^{\frac{3}{2}}) + K_2\lambda_n^{\frac{1}{3}}\sqrt{\zeta}J_{-\frac{1}{3}}(\tfrac{2}{3}\lambda_n\zeta^{\frac{3}{2}}). \quad (7)$$

The coefficients K_1, K_2 and the eigenvalues λ_n are obtained by applying the boundary conditions, and the A_n in equation (6) are obtained from the entry condition using the usual orthogonality properties of $\Psi_n(\zeta)$ and $\Psi_m(\zeta)$.

EXPERIMENTS

The experimental equipment used in this work is essentially the same as that described in [7], however, the heat transfer test section was redesigned to eliminate axial conduction in the wall [44]. Air, supplied by a turbo-compressor, was cooled and saturated in a spray chamber, passed through a plenum chamber and through a section containing tubes to straighten the flow, then flowed through a converging section which served as a venturi to measure the flow rate. The test section, a 6·1 m long plexiglas wind tunnel 25 cm in width by 2·61 cm in height, was connected to the venturi by means of a flexible rubber section to minimize vibration. A metered (by rotameters) stream of water was introduced through perforations in the tunnel bottom near the air inlet.

The heat transfer section consisted of a 60·1 cm copper block inserted flush with the tunnel bottom and extending the width of the tunnel. The upstream edge of the block was 4·9 m from the air inlet. The copper block was cut into 6 sections as indicated in Fig. 2, and the sections were insulated from each other by 1·6 mm thick Teflon sheets. As will be shown, the axial conduction in the block produced by variations in the surface temperature of the block due to heat transfer to the liquid film was effectively eliminated by cutting and insulating the block. Since axial conduction would be most pronounced near the upstream edge of the block, the sections were shortest near the leading edge, increasing in length as one proceeds downstream. Electrical strip heaters were installed beneath the copper block, each set of heaters being controlled by separate variable transformers. The electrical power supplied to

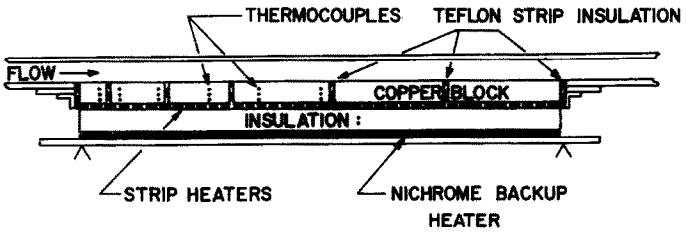

FIG. 2. The heat transfer test section.

each section was measured using calibrated voltmeters and ammeters. With this arrangement either constant and uniform wall temperatures or constant uniform heat flux boundary conditions could be maintained. For all of the data reported below the constant flux boundary condition was used.

The energy supplied to the film was generally kept at a low enough level to prevent a large increase in the mixed mean fluid temperature across the heat transfer test section. This had two desired effects (1) to keep the transverse temperature gradients in the film small enough to prevent instabilities due to buoyant forces and (2) to eliminate the effects of variable physical properties on the heat transfer. When the liquid

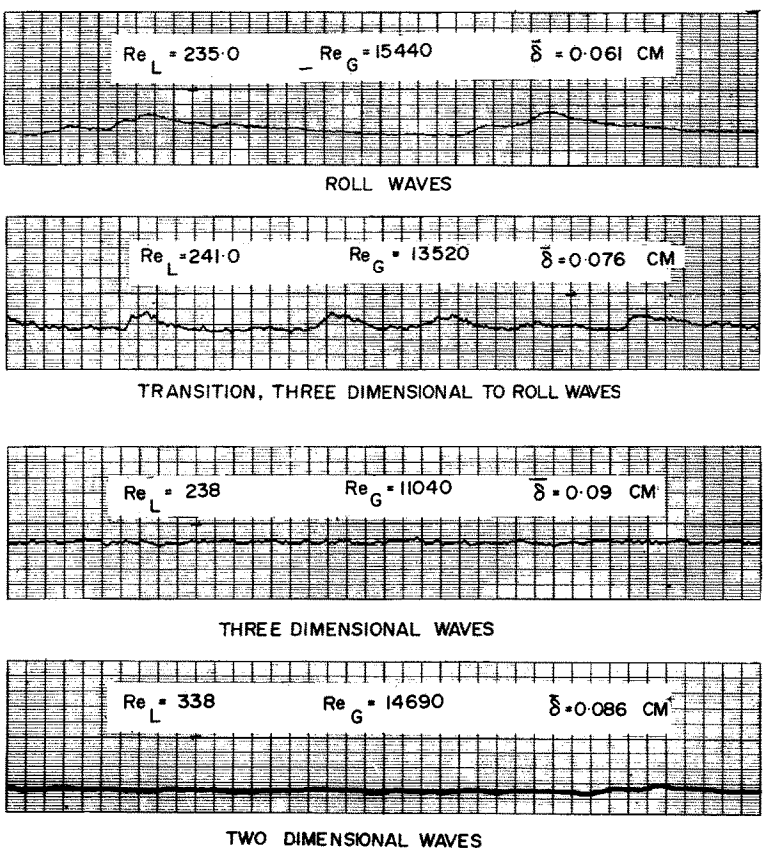

FIG. 3. Oscillograph tracings of wave characteristics.

flow rate was very low, however, the first effect could not always be avoided because the heat flux required was too low to measure accurately. At very low heat fluxes ($q_w < 9000$ J/m^{2}s) the error in the energy balance (power input compared with the enthalpy increase of the liquid film) on the liquid film was unacceptably high (error > 10 per cent).

The film thicknesses were measured by means of the micrometer probe and the conductance cells (platinum electrodes mounted flush with the tunnel bottom) described in [5] and [7]. Typical oscillograph tracings of the cell output are shown in Fig. 3. Other measurements and details are discussed in a thesis by Frisk [45].

To directly determine the differences in heat transfer characteristics between smooth film and wavy film conditions experiments were carried out as follows: Gas and liquid flow rates were set such that some desired flow regime was attained. The power to the heaters was turned on, adjusted to constant wall heat flux conditions, and the system was permitted to reach steady state. The temperature distribution in the copper block and the various fluid mechanics and thermal parameters were then measured. When the measurements were complete the system was maintained at exactly the same flow rates and power levels and surfactant was added to the liquid phase collecting tank at the wind tunnel exit. The recirculation of the liquid phase led to thorough mixing of the soluble surfactant (Kodak Photo Flow-200), and within a few minutes the wave motion in the test section was usually completely suppressed.

RESULTS

For tap water uncontaminated with surfactant the flow regimes described above were observed. Figure 4 is a flow map for uncon-

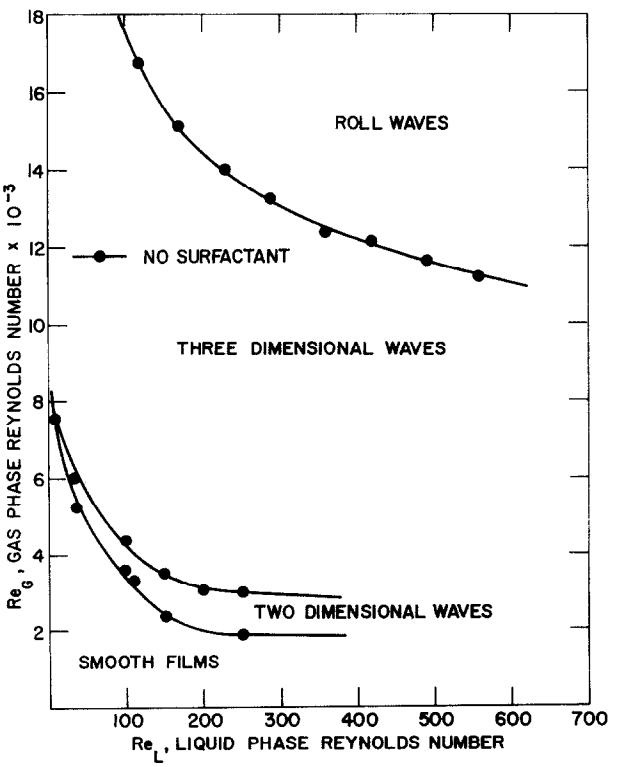

FIG. 4. Flow regimes for uncontaminated water.

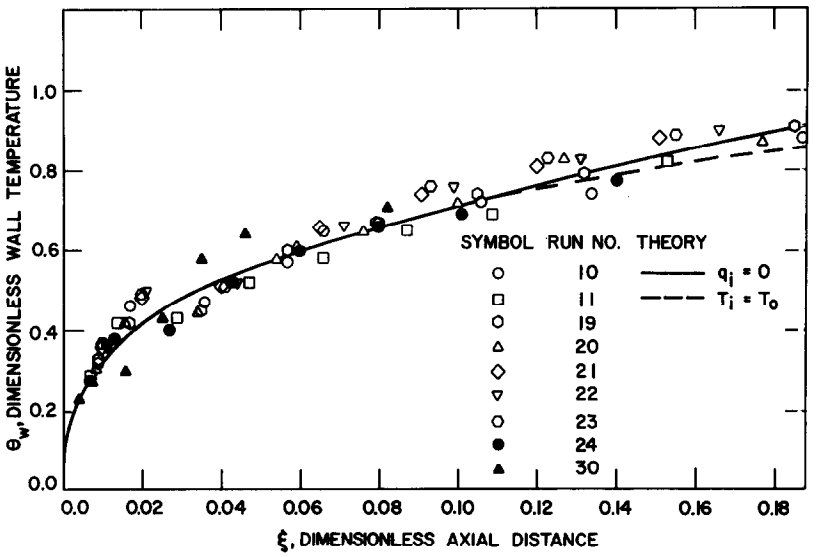

FIG. 5. A comparison between experimental and theoretical wall temperature profiles for smooth liquid film flow.

taminated water showing the transitions to two- and three-dimensional waves and to roll waves as functions of the gas and liquid Reynolds numbers. The two-dimensional regime is seen to exist over a rather small region of gas and liquid flow rates, but the three-dimensional structure occurs over a much wider range. By adding surfactant to the liquid it was always possible to suppress two- and three-dimensional waves, but the roll wave transition is only slightly affected by surface-active agents, so it was necessary to operate only slightly above the roll wave transition line of Fig. 4 if roll waves were to be stabilized.

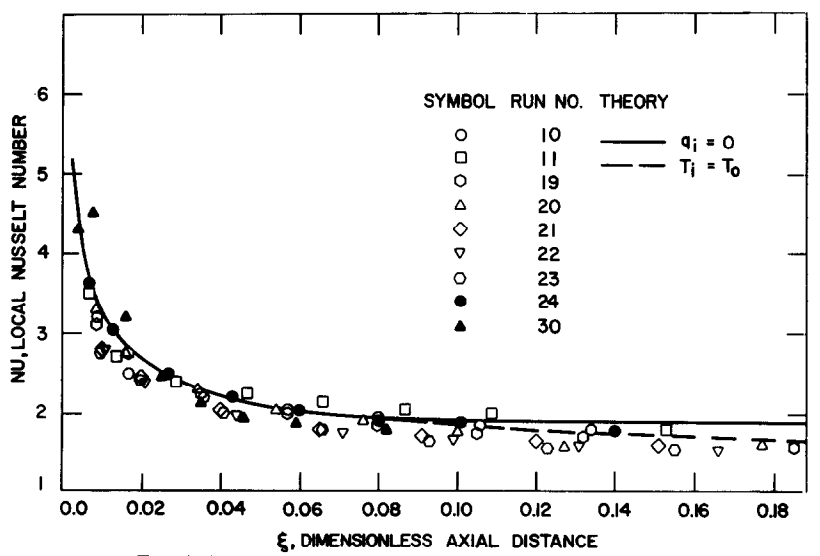

FIG. 6. A comparison between experimental and theoretical Nusselt numbers for smooth liquid film flow.

The heat transfer results for the smooth film runs are in excellent agreement with the analysis of Davis and Cooper as seen in Figs. 5 and 6. Figure 5 is a plot of the dimensionless wall temperature versus dimensionless axial position. The theoretical results for an adiabatic interface (no heat transfer to the gas phase) and for a constant interfacial temperature are both plotted. Figure 6 is a similar comparison between the theoretical and experimental Nusselt numbers as a function of the dimensionless axial position. The Nusselt number is defined by

$$Nu \equiv \frac{q_w \delta}{k(T_w - T_b)}$$

where q_w and δ are the measured local heat flux and measured film thickness, respectively. The local wall temperature T_w was measured by extrapolating the temperature profiles in the copper block to the solid surface and the local mixed mean liquid temperature T_b was calculated knowing the liquid flow rate, inlet temperature and heat capacity and the power input up to the axial position in question.

The experimental results summarized in Figs. 5 and 6 generally fall within the thermal entry region where the temperature distributions are not fully developed. A measure of the thermal entry length is the point at which the theoretical solutions for constant interfacial temperature and for an adiabatic interface begin to diverge. For $\xi < 0{\cdot}08$ the wall temperature axial profiles and the Nusselt number profiles are independent of the interfacial boundary condition, for the thermal boundary layer is still thinner than the liquid film. The Nusselt number results for $\xi < 0{\cdot}08$ suggest that a constant interfacial temperature is the proper boundary condition here.

The flow parameters and other information

Table 1. Summary of experimental parameters

Run No.	Film	Re_{L_i}	Re_L	Re_G	u_i (cm/s)	δ (cm)	Po	σ (dyne/cm)	Gr/Re_{L_i}	q_w (J/m²s)	$\bar{h}$ (J/m²s°K)
7	Smooth	156	104	2540	7·8	0·213	0·035	—	1·25	9150	870
8	Smooth	154	106	2800	7·8	0·206	0·043	—	1·15	9110	880
9	Smooth	139	102	2840	7·4	0·203	0·043	—	1·23	9130	800
10	Smooth	368	242	15540	44·5	0·094	0·032	49·00	0·07	21170	1230
11	Smooth	417	248	14720	44·5	0·104	0·036	49·00	0·09	21300	1220
12	Roll waves	367	243	15370	44·5	0·094	0·062	—	—	21030	2580
13	Roll waves	410	243	14700	44·5	0·104	0·047	—	—	20610	2300
14	3D-patches	341	244	13060	36·9	0·104	0·044	—	—	20920	2120
15	3D waves	328	246	10960	32·1	0·114	0·045	—	—	20830	1910
16	Roll waves	370	262	18540	69·5	0·056	0·016	—	—	21210	3250
17	2D waves	371	257	2810	12·4	0·320	0·069	—	—	18820	890
18	Smooth	374	259	2780	12·4	0·320	0·068	55·51	3·68	18640	900
19	Smooth	358	239	12450	36·9	0·104	0·031	56·68	0·12	18940	1090
20	Smooth	345	242	10550	32·1	0·114	0·034	56·68	0·18	18280	990
21	Smooth	383	240	15770	49·8	0·084	0·024	46·77	0·05	20920	1250
22	Smooth	338	239	14690	42·8	0·086	0·025	46·77	0·07	21010	1180
23	Smooth	333	235	13720	40·6	0·091	0·026	50·72	0·07	18580	1100
24	Smooth	369	234	11230	32·5	0·127	0·043	50·72	0·21	19000	990
25	Roll waves	375	235	15740	49·8	0·084	0·032	—	—	21220	2540
26	Roll waves	333	235	14600	42·8	0·086	0·033	—	—	21130	2440
27	3D-RW trans	342	241	13520	40·6	0·091	0·034	—	—	18710	2300
28	3D waves	376	238	11040	32·5	0·127	0·057	—	—	18640	1990
29	3D waves	427	228	8540	26·8	0·183	0·087	—	—	9450	1310
30	Smooth	430	230	8690	26·8	0·183	0·072	59·74	0·36	9180	770
31	2D-3D trans	455	225	4190	16·9	0·312	0·091	—	—	9260	650
32	Smooth	455	225	4190	16·9	0·312	0·093	59·74	1·84	9310	630
33	Roll waves	334	248	17220	59·5	0·058	0·017	—	—	20940	2720

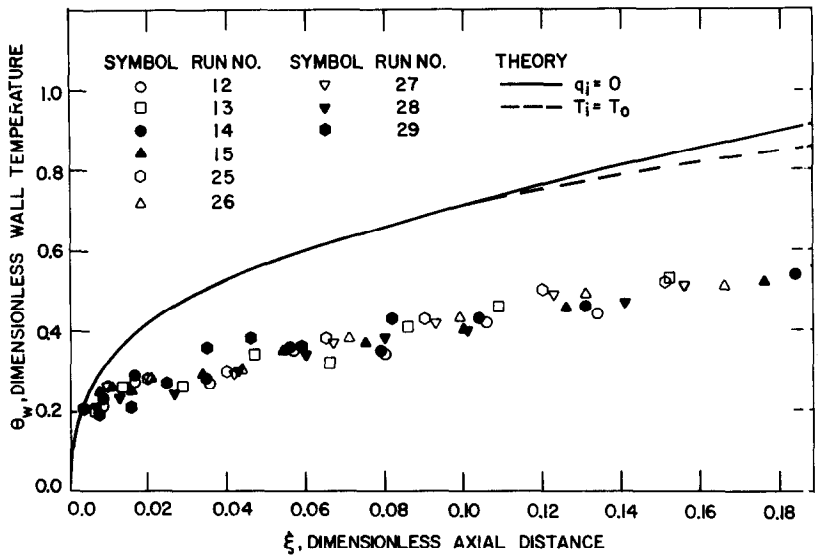

FIG. 7. The effects of wavy liquid flow on the wall temperature profile.

for the experimental runs are summarized in Table 1. The data shown in Figs. 5 and 6 represent a fairly wide range of smooth film conditions.

The Nusselt number results of Fig. 6 are in much better agreement with theory than the results of Davis and Cooper because the effects of axial conduction in the wall have been eliminated here. Axial conduction in the wall tends to increase the wall temperature in the upstream region of the block, thereby, reducing the calculated Nusselt number.

The effects of three-dimensional waves and roll waves on the heat transfer characteristics are shown in Figs. 7 and 8. The local Nusselt numbers and the dimensionless distances ξ

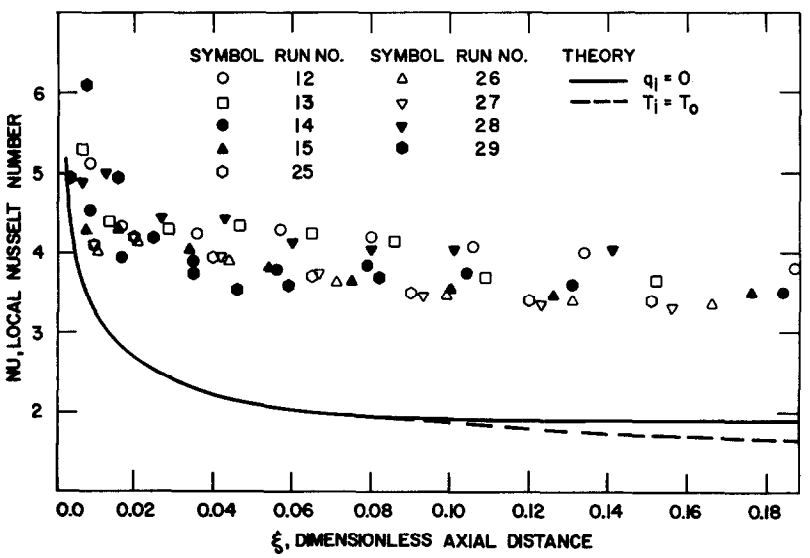

FIG. 8. The effects of wavy liquid flow on the local Nusselt numbers.

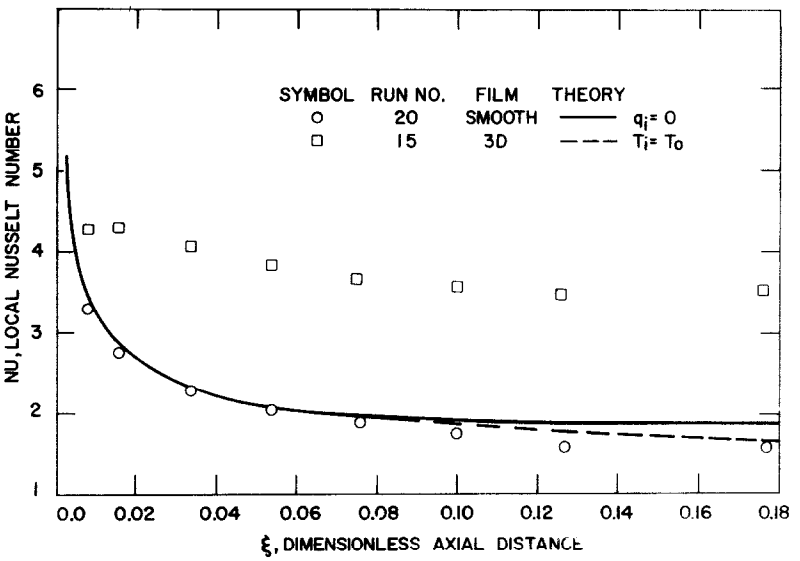

FIG. 9. A comparison between heat transfer results for smooth film flow and three-dimensional wave flow.

calculated for these runs are based on the properties of the corresponding smooth film runs for which the flow was stabilized using a surface-active agent. In this way the results can be directly compared with the theory for smooth film flow. Figure 7 shows that the wall temperatures are considerably lower than those predicted for smooth film flow. Furthermore, the wall temperature is nearly linear in ξ for these data, suggesting that the fully developed temperature profiles are reached within a short distance from the leading edge.

The local Nusselt numbers are generally much higher than those predicted for smooth films. For most of the runs shown the heat transfer enhancement is nearly 100 per cent.

A sharper contrast between smooth and wavy flow data is obtained by comparing the run pairs for which the only difference in conditions is the presence of surfactant in the liquid for one of the runs. Figure 9 is a comparison between the Nusselt numbers for run 20, which involved a smooth contaminated film, and run 15, which involved a three-dimensional wave structure, at otherwise identical conditions. Figure 10 is a similar comparison between a smooth film flow and roll waves.

The nearly step-like decrease in the Nusselt number for $0{\cdot}01 < \xi < 0{\cdot}02$ shown in Fig. 10 suggests that the thermal entry length is very short for roll waves. The turbulent eddies that precede the wave crests apparently penetrate nearly to the wall. It is rather interesting to note that although roll waves appear to be more turbulent than three-dimensional waves the heat transfer enhancement associated with roll waves is not significantly greater than for three-dimensional waves.

When only trace amounts of surfactants are used two- and three-dimensional wave regimes may be replaced by wave patches, which involve patches of three-dimensional waves scattered over an otherwise smooth surface. The surface may even alternate between three-dimensional waves and wave patches in a very irregular manner. Figure 11 shows a comparison between Nusselt numbers for such an irregular flow and for the corresponding smooth flow. As in the case of roll waves and regular three-dimensional waves the Nusselt number is increased by a

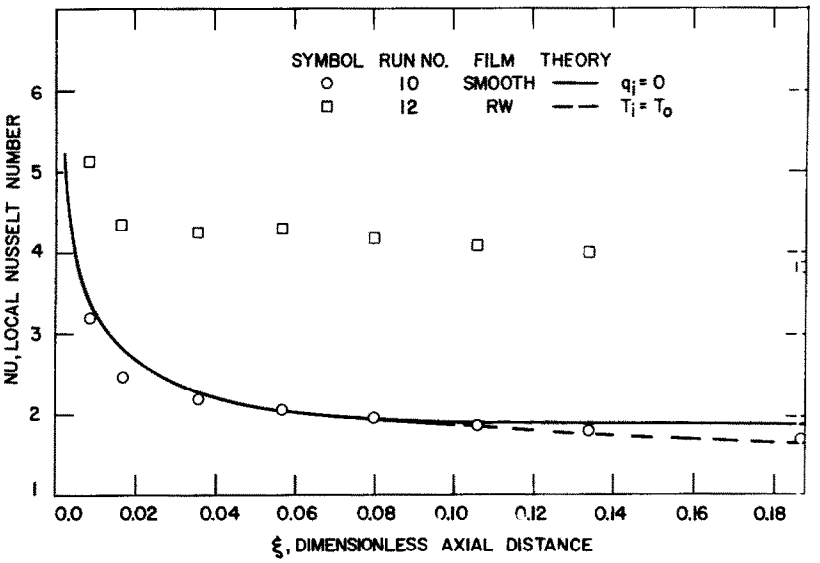

FIG. 10. A comparison between heat transfer results for smooth film flow and roll waves.

factor of about 2 compared with smooth films.

Two-dimensional waves exist only at relatively low gas and liquid Reynolds numbers, and the heat transfer data taken at low Reynolds numbers show some unexpected results. Figure 12 shows these results for some smooth film data. In the upstream portion of the heated film the Nusselt numbers follow the theoretical predictions, but at some point down-stream from the leading edge of the heated wall (which de-

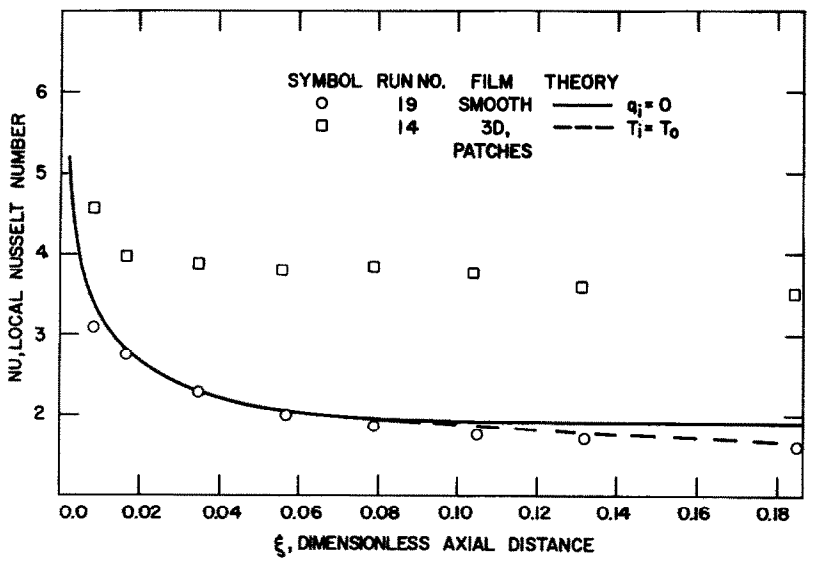

FIG. 11. A comparison between heat transfer results for smooth film flow and waves in the transition from three-dimensional waves to wave patches.

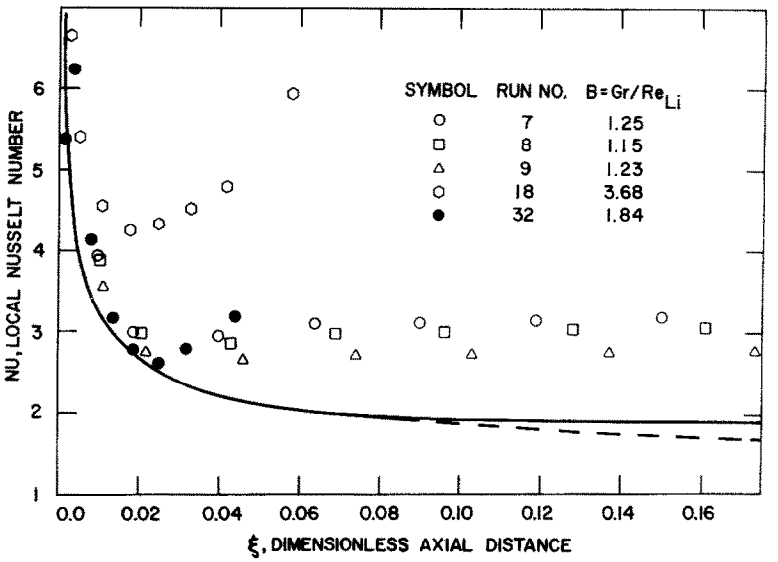

FIG. 12. Nusselt numbers for two-dimensional wave flow.

pends on the heat flux as well as the flow rates) a minimum Nusselt number is attained followed by a sudden increase in Nu. Since the apparent transition is affected by the heat flux as well as the flow rate a Rayleigh-like instability is suggested. If we examine the ratio of the Grashoff to Reynolds numbers for all of the runs taken (see Table 1) it becomes clear that the sudden increase in Nu is due to the onset of natural convection. Defining the relevant Grashoff number as $Gr \equiv \delta^3 \rho_L^2 g\beta(T_w - T_b)/\mu_L^2$ and the Reynolds number based on the interfacial

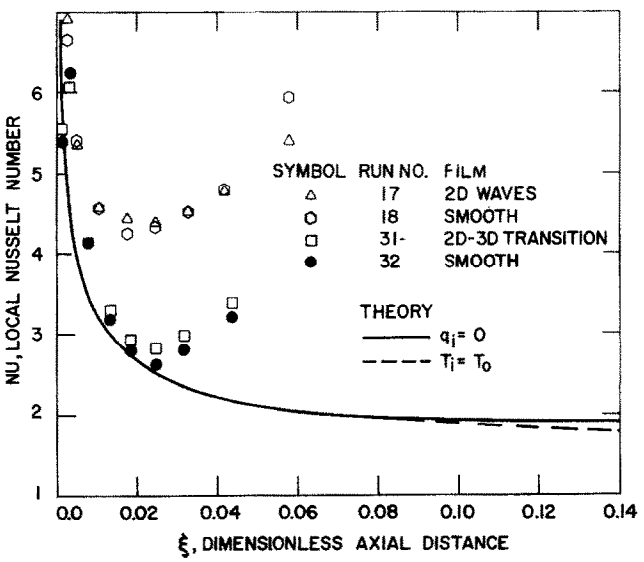

FIG. 13. A comparison between heat transfer results for smooth film flow and the corresponding two-dimensional waves.

velocity as $Re_{L_i} \equiv \delta U_i/\nu_L$, the ratio $B \equiv Gr/Re_{L_i}$ is given on Fig. 12 and in Table 1. For the great majority of the experimental runs $B \ll 1$, but for all of the runs exhibiting a minimum Nu we have $B > 1$. For runs 17 and 18, which show the most pronounced effects of natural convection $B = 3{\cdot}68$, the highest value of B attained. As B decreases the Nusselt numbers approach those predicted for smooth films.

Although the two-dimensional runs exhibited a minimum Nu, comparisons can be made between results for smooth films and two-dimensional wavy films. The results are shown on Fig. 13. There are no significant differences between runs 17 and 18 and between 31 and 32. Although natural convection effects could mask any differences between runs 17 and 18 due to waves, the data for the upstream region of the heater for runs 31 and 32 are significant. There is no measurable difference between runs 31 and 32, which were taken precisely at the same flow conditions. Before and after the surfactant was added during the course of these runs no wall temperature changes nor any other thermal effects were observed. The only effect was damping of the two-dimensional ripples after surfactant was added.

As indicated in Table 1 the Poiseuille number for all runs was sufficiently low ($Po \leqslant 0{\cdot}093$) that the liquid phase velocity profile may be considered to be linear. The static surface tensions, measured after each run, are reported for those runs involving surface-active agent. For the other runs $\sigma = 74{\cdot}4$ dyne/cm, which is usual for uncontaminated water.

One further comparison among the heat transfer results can be made that is very informative. We can compare the average heat transfer coefficient $\bar{h}$ for all of the runs measured at a particular liquid flow rate (or volumetric Reynolds number). We shall define $\bar{h}$ as the heat transfer coefficient averaged over the heat transfer surface between the first and last thermocouple stations, i.e.

$$\bar{h} \equiv \frac{1}{x_8 - x_1} \int_{x_1}^{x_8} h \, dx. \tag{8}$$

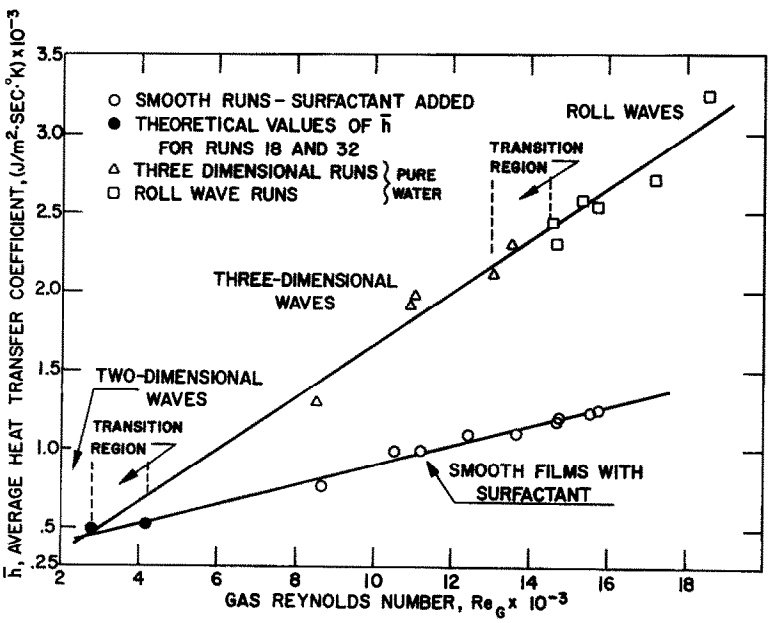

FIG. 14. Average heat transfer coefficients as a function of the flow regime and the gas phase Reynolds number.

The results for $Re_L = 240 \pm 9$ per cent are shown in Fig. 14 as $\bar{h}$ vs. Re_G. The data for smooth films and the two-dimensional waves data (calculated by assuming that the points beyond the onset of natural convection lie on the smooth film curve of Fig. 13) lie on a single straight line, and the other wavy film data lie on a second straight line of greater slope than that for the smooth data. By using the method of least squares nearly the same upper line is obtained whether one uses only the three-dimensional wave data or only the roll wave data. This is somewhat surprising because of the markedly different appearance of the two regimes. The three-dimensional waves appear to be merely surface waves that do not penetrate to the solid wall whereas the roll waves, though there are three-dimensional waves on their surfaces, appear to be quite turbulent just downstream of the crests. The surging, unsteady nature of the roll waves does not show up in the heat transfer measurements because of the large thermal capacity of the copper block, so it is possible that any change in the heat transfer characteristics associated with the roll wave transition is masked by the heat capacity of the block.

CONCLUSIONS

(1) Experimental Nusselt numbers and wall temperatures for heat transfer to smooth horizontal liquid films are in good agreement with theoretical predictions.

(2) Two-dimensional ripples have no effect on heat transfer at the wall in the thermal entry region.

(3) Three-dimensional and roll waves can increase the Nusselt numbers by more than 100 per cent compared with smooth film flow.

(4) For $Gr/Re_{L_i} > 1$ the thin liquid films are unstable with respect to buoyant forces due to density gradients in the film. Natural convection in the film was found to occur in the downstream portion of the test section for $Gr/Re_{L_i} > 1$.

ACKNOWLEDGEMENTS

The authors are grateful to the National Science Foundation for Grant GK 10269. The present work was carried out under that grant. The authors also wish to acknowledge the assistance of T. V. Narasimhan who helped construct the equipment and collect the data.

REFERENCES

1. T. J. Hanratty and J. M. Engen, Interaction between a turbulent air stream and a moving water surface, *A.I.Ch.E. Jl* **3**, 299–304 (1957).
2. S. R. M. Ellis and B. Gay, The parallel flow of two fluid streams: interfacial shear and fluid–fluid interaction, *Trans. Inst. Chem. Engrs* **37**, 206–213 (1959).
3. J. J. van Rossum, Experimental investigation of horizontal liquid films. Wave formation, atomization, film thickness, *Chem. Engng Sci.* **11**, 35–52 (1959).
4. T. N. Smith and R. W. F. Tait, Interfacial waves in horizontal gas–liquid flow, *Aust. J. Appl. Sci.* **15**, 247–260 (1964).
5. E. J. Davis, Interfacial shear measurement for two-phase gas–liquid flow by means of Preston tubes, *I/EC Fundamentals* **8**, 153–159 (1969).
6. T. J. Hanratty and A. Hershman, Initiation of roll waves, *A.I.Ch.E. Jl* **7**, 488–497 (1961).
7. E. J. Davis and T. J. Cooper, Thermal entrance effects in stratified gas–liquid flow: experimental investigation, *Chem. Engng Sci.* **24**, 509–520 (1969).
8. A. D. D. Craik, Wind-generated waves in contaminated liquid films, *J. Fluid Mech.* **31**, 141–161 (1968).
9. F. I. P. Smith and A. D. D. Craik, Wind-generated waves in thin liquid films with soluble contaminant, *J. Fluid Mech.* **45**, 527–544 (1971).
10. T. V. Narasimhan, A study of surface waves in stratified gas–liquid flow, M.S. Thesis, Clarkson College of Technology (1971).
11. T. V. Narasimhan and E. J. Davis, Surface waves and surfactant effects in stratified gas–liquid flow, submitted for publication.
12. R. E. Emmert and R. L. Pigford, A study of gas absorption in falling liquid films, *Chem. Engng Prog.* **50**(2), 87–93 (1954).
13. W. Brotz, Uber die Vorausberechnung der Absorptionsgeschurndigkeit von Gasen in Stromenden Flussigkeitsschichten, *Chem.-Ing.-Tech.* **26**, 470–478 (1954).
14. S. Kamei and J. Oishi, Mass and heat transfer in a falling liquid film of wetted wall tower, *Mem. Fac. Engng, Kyoto Univ.* **17**, 227–239 (1955).
15. C. Stirba and D. M. Hurt, Turbulence in falling liquid films, *A.I.Ch.E. Jl* **1**, 178–184 (1955).
16. H. Kramers and P. J. Kreyger, Mass transfer between a flat surface and a falling liquid film, *Chem. Engng Sci.* **6**, 42–48 (1956).
17. E. Ruckenstein and C. Berbente, Mass transfer in wave flow, *Chem. Engng Sci.* **20**, 795–801 (1965).
18. W. Malewski, Zusammenhang Zwischen Stoffübergang und Wellenstrucktur beim Welligen Rieselfilm, *Chemie. Ingr. Tec.* **37**, 815–825 (1965).
19. C. J. King, Turbulent liquid phase mass transfer at a free gas–liquid interface, *I/EC Fundamentals* **5**, 1–8 (1966).

20. D. P. BOYD and J. M. MARCHELLO, Role of films and waves on gas absorption, *Chem. Engng Sci.* **21**, 769–776 (1966).
21. J. C. JEPSEN, O. K. CROSSER and R. H. PERRY, The effect of wave induced turbulence on the rate of absorption of gases in falling liquid films, *A.I.Ch.E. Jl* **12**, 186–192 (1966).
22. F. P. STAINTHORP and G. J. WILD, Film flow—the simultaneous measurement of wave amplitude and the local mean concentration of a transferable component, *Chem. Engng Sci.* **22**, 701–704 (1967).
23. S. BANERJEE, E. RHODES and D. S. SCOTT, Mass transfer to falling wavy liquid films at low Reyonlds numbers, *ibid.* **22**, 43–48 (1967).
24. A. IRIBARNE, A. D. GOSMAN and D. B. SPALDING, A theoretical and experimental investigation of diffusion-controlled electrolytic mass transfer between a falling liquid film and a wall, *Int. J. Heat Mass Transfer* **10**, 1661–1676 (1967).
25. S. BANERJEE, D. S. SCOTT and E. RHODES, Mass transfer to falling wavy liquid films in turbulent flow, *I/EC Fundamentals* **7**, 22–27 (1968).
26. R. Z. TUDOSE, T. SAVEANU and G. CRISTIAN, Transfer processes between immiscible liquids. The hydrodynamics of film flow, *Int. Chem. Engng* **7**, 637–642 (1967).
27. S. L. GOREN and R. V. S. MANI, Mass transfer through horizontal liquid films in wavy motion, *A.I.Ch.E. Jl* **14**, 57–60 (1968).
28. D. W. HOWARD and E. N. LIGHTFOOT, Mass transfer to falling films: Part 1. Application of the surface-stretch model to uniform wave motion, *ibid.* **14**, 458–467 (1968).
29. M. F. GALIULLIN and P. A. SEMENOV, Mass transfer in thin liquid films during upward flow, *Theor. Found. Chem. Engng* **2**, 143–148 (1968).
30. KR. BOYADZHIEV, V. LEVICH and V. KRYLOV, The effect of surface active materials on mass transfer in laminar film flow. I. Improvement of the theory of convective diffusion, *Int. Chem. Engng* **8**, 393–396 (1968).
31. YU. I. DYTNERSKII and N. S. BREKHOVSKIKH, Some problems of CO_2 absorption by water flowing as a film, *Theor. Found. Chem. Engng* **2**, 711–714 (1968).
32. K. B. BOYADZHIEV, Effect of surface-active substances on absorption rate of sparingly soluble gases by laminar liquid film, *ibid.* **2**, 581–586 (1968).
33. E. RUCKENSTEIN and C. BERBENTE, Mass transfer to falling liquid films at low Reynolds numbers, *Int. J. Heat Mass Transfer* **11**, 743–753 (1968).
34. A. A. WRAGG, P. SERAFIMIDIS and A. EINARSSON, Mass transfer between a falling liquid film and a plane vertical surface, *Int. J. Heat Mass Transfer* **11**, 1287–1289 (1968).
35. D. R. OLIVER and T. E. ATHERINOS, Mass transfer to liquid-films on an inclined plane, *Chem. Engng Sci.* **23**, 525–536 (1968).
36. L. P. KHOLPANOV, V. YA. SHKADOV, V. A. MALYUSOV and N. M. ZHAVORONKOV, Mass transfer in a liquid film during wave formation (linear velocity distribution), *Theor. Found. Chem. Engng* **3**, 386–389 (1969).
37. G. S. BAYS and W. H. MCADAMS, Heat transfer coefficients in falling film heaters, *Ind. Engng Chem.* **29**, 1240–1246 (1937).
38. A. G. WILLIAMS, S. S. NANDAPURKAR and F. A. HOLLAND, A review of methods for enhancing heat transfer rates in surface condensers, *The Chem. Engr* n223, CE367–CE373 (1968).
39. R. CHAND and H. F. ROSSON, Local heat flux to a water film flowing down a vertical surface, *I/EC Fundamentals* **4**, 356–359 (1965).
40. I. M. FEDOTKIN and V. R. FIRISYUK, Heat transfer rates along a surface wetted by a thin liquid film, *Heat Transfer Soviet Res.* **1**, 115–122 (1969).
41. H. Y. CHOI, Electrohydrodynamic condensation heat transfer, *J. Heat Transfer* **90**, 98–102 (1968).
42. E. E. O'BRIEN, On the flux of heat through laminar wavy liquid layers, *J. Fluid Mech.* **28**, 295–303 (1967).
43. E. J. DAVIS, Exact solutions to a class of heat and mass transfer problems, *Brit. Chem. Engng*, in press.
44. E. J. DAVIS and W. N. GILL, The effects of axial conduction in the wall on heat transfer with laminar flow, *Int. J. Heat Mass Transfer* **13**, 459–470 (1970).
45. D. P. FRISK, The enhancement of heat transfer by waves in stratified gas–liquid flow, M.S. Thesis, Clarkson College of Technology (1971).

L'AUGMENTATION DU TRANSFERT THERMIQUE PAR DES ONDES DANS L'ÉCOULEMENT STATIFIÉ GAZ-LIQUIDE

Résumé—Une recherche expérimentale sur le transfert thermique d'une plaque plane à un écoulement horizontal air-eau cocourant a été réalisée pour évaluer les effets de régimes d'écoulement différents sur l'efficacité du transfert thermique. Les résultats pour l'écoulement d'un film liquide lisse et pour un écoulement de la phase liquide avec ondes bidimensionnelles sont en accord avec l'analyse théorique du transfert thermique relatif à des films lisses. Des ondes tridimensionnelles et des rouleaux accroissent de plus de 100% le nombre de Nusselt (comparé aux films lisses). En utilisant un agent tensio-actif pour stabiliser l'écoulement on obtient une comparaison directe entre le transfert thermique avec écoulement ridé et le transfert thermique avec écoulement lisse. Il se produit une instabilité de type Rayleigh due aux forces d'Archimède pour des valeurs suffisamment basses du nombre de Reynolds de la phase gazeuse et des flux thermiques à la paroi suffisamment élevés.

DIE ERHÖHUNG DER WÄRMEÜBERTRAGUNG DURCH WELLEN IN GESCHICHTETER GAS–FLÜSSIGKEITS-STRÖMUNG.

Zusammenfassung—Die Wärmeübertragung von einer ebenen Platte auf eine horizontale, gleichgerichtete Luft–Wasser–Strömung wurde experimentell untersucht, um die Auswirkungen verschiedener Strömungsbedingungen auf die Effektivität der Wärmeübertragung abzuschätzen. Es wird gezeigt, dass die Ergebnisse für glatten Flüssigkeitsfilm und für zweidimensionale, wellige Strömung der flüssigen Phase mit der theoretischen Analyse der Wärmeübertragung für glatten Flüssigkeitsfilm übereinstimmen. Dreidimensionale Wellen und Rollwellen bewirken eine Erhöhung der Nusselt-Zahl (im Vergleich zum glatten Flüssigkeitsfilm) von über 100%. Durch Verwendung oberflächenaktiver Mittel zur Stabilisierung der Strömung kann ein direkter Vergleich zwischen der Wärmeübertragung bei welliger und glatter Strömung erzielt werden. Es wird gezeigt, dass bei genügend kleiner Reynolds-Zahl der flüssigen Phase und ausreichend hohem Wärmefluss durch die Wand Rayleigh-ähnliche Instabilitäten infolge von Auftriebskräften auftreten.

ИНТЕНСИФИКАЦИЯ ТЕПЛООБМЕНА ВОЛНАМИ В СТРАТИФИЦИРОВАННОМ ГАЗО-ЖИДКОСТНОМ ПОТОКЕ

Аннотация—Для того чтобы определить влияние различных режимов течения на эффективность теплообмена, проводилось экспериментальное исследование переноса тепла от плоской пластины к горизонтальному воздушно-водяному потоку. Показано, что результаты экспериментального исследования плавного течения жидкой пленки и двумерного волнового течения согласуются с результатами теоретического анализа переноса тепла при плавном течении. Показано также, что по сравнению с плавным течением трехмерные волны и закрученные волны повышают число Нуссельта более, чем на 100%.

Используя поверхностно-активное вещество для стабилизации течения, проведено сравнение теплообмена при волновом течении с теплообменом при плавном течении. Показано, что при достаточно низких значениях числа Рейнольдса газовой фазы и довольно высоких тепловых потоках на стенке имеет место неустойчивость типа Релея, вызванная действием подъемных сил.